NeuroImage: Clinical 36 (2022) 103159

Contents lists available at ScienceDirect

NeuroImage: Clinical

journal homepage: www.elsevier.com/locate/ynicl

^{1}H-MRS neurometabolites and associations with neurite microstructures and cognitive functions in amnestic mild cognitive impairment

Elveda Gozdas [a,*], Lauren Hinkley [a], Hannah Fingerhut [a], Lauren Dacorro [a], Meng Gu [b], Matthew Sacchet [c], Ralph Hurd [b], S.M. Hadi Hosseini [a]

[a] Department of Psychiatry and Behavioral Sciences, Stanford University School of Medicine, Stanford, CA, USA
[b] Department of Radiology, Stanford University, Stanford, CA, USA
[c] Center for Depression, Anxiety, and Stress Research, McLean Hospital, Harvard Medical School, Belmont, MA, USA

ARTICLE INFO

Keywords:
Dorsolateral prefrontal cortex
Alzheimer's disease
Magnetic resonance spectroscopy
Neurite microstructures

ABSTRACT

Alzheimer's disease (AD) pathogenesis is associated with alterations in neurometabolites and cortical microstructure. However, our understanding of alterations in neurochemicals in the prefrontal cortex and their relationship with changes in cortical microstructure in AD remains unclear. Here, we studied the levels of neurometabolites in the left dorsolateral prefrontal cortex (DLPFC) in healthy older adults and patients with amnestic Mild Cognitive Impairments (aMCI) using single-voxel proton-magnetic resonance spectroscopy (^{1}H-MRS). *N*-acetyl aspartate (NAA), glutamate+glutamate (Glx), Myo-inositol (mI), and γ-aminobutyric acid (GABA) brain metabolite levels were quantified relative to total creatine (tCr = Cr + PCr). aMCI had significantly decreased NAA/tCr, Glx/tCr, NAA/mI, and increased mI/tCr levels compared with healthy controls. Further, we leveraged advanced diffusion MRI to extract neurite properties in the left DLPFC and found a significant positive correlation between NAA/tCr, related to neuronal intracellular compartment, and neurite density (ICVF, intracellular volume fraction), and a negative correlation between mI/tCr and neurite orientation (ODI) only in healthy older adults. These data suggest a potential decoupling in the relationship between neurite microstructures and NAA and mI concentrations in DLPFC in the early stage of AD. Together, our results confirm altered DLPFC neurometabolites in prodromal phase of AD and provide unique evidence regarding the imbalance in the association between neurometabolites and neurite microstructure in early stage of AD.

1. Introduction

Alzheimer's disease is an irreversible, disabling neurodegenerative disease with a long preclinical phase. Mild Cognitive Impairment (MCI) is the transient state of AD that has been defined by the onset of initial mild cognitive symptoms accompanied by neurobiological changes that may eventually lead to neurodegeneration. Preventing the future impact of AD depends on identifying individuals at risk, determining predictors of progression, and providing early treatment during the prodromal stage such as MCI. Amyloid beta (Aβ) and tau imaging can be used to detect the preclinical pathology of AD using an advanced molecular imaging method, positron emission tomography (PET) (Dubois et al., 2021; Maschio and Ni, 2022). However, the pathogenesis of AD is not limited to Aβ plaques and tau tangles but also includes changes in neurochemical characteristics of the brain. Proton magnetic resonance spectroscopy (1H-MRS) is another molecular quantification technique that can be used to measure the alterations in the levels of endogenous brain neurochemicals that could be indicative of the disease processes (Mitolo et al., 2019).

1H-MRS is a non-invasive method that uses the radiofrequency electromagnetic signals of the atomic nuclei in different molecules to quantify the concentration of brain neurometabolites within specific regions (Novotny et al., 1998). Most of the studies have determined that regional changes in the levels of *N*-acetyl-aspartate (NAA), myoinositol (mI), glutamate-glutamine complex (Glx), and gamma-aminobutyric acid (GABA) may be potential biomarkers of disease progression in aMCI and AD patients (Olson et al., 2008; Gao and Barker 2014; Waragai et al., 2017; Govindpani et al., 2020). To date, the studies examining metabolite concentrations in aMCI and AD looked at these concentrations in the posterior cingulate cortex (PCC), anterior cingulate cortex (ACC), hippocampus and medial-temporal lobe (Jones and Waldman, 2004; Jessen et al., 2009; Kantarci 2013; Oeltzschner et al., 2019)

* Corresponding author at: Department of Psychiatry and Behavioral Sciences, CBRAIN Lab, 401 Quarry Rd., Stanford, CA 94305-5795, USA.
E-mail address: elvedags@stanford.edu (E. Gozdas).

https://doi.org/10.1016/j.nicl.2022.103159
Received 8 April 2022; Received in revised form 4 August 2022; Accepted 18 August 2022
Available online 22 August 2022

because the early stage of AD is characterized by memory disturbances that result from neurodegeneration in the parietal and medial temporal cortices (Squire et al., 2004; Dubois et al., 2021). However, recent data suggest the importance of the prefrontal cortex (PFC) in memory processes through various direct and indirect connections with medial temporal structures (Eichenbaum, 2017). It has also been extensively reported that the PFC has a central role in working memory and executive functioning (Spellman et al., 2015), both of which are significantly impaired in early AD and AD patients (Salat et al., 2001; Van Veluw et al., 2012; Jung et al., 2020). The deficits in PFC plasticity are also correlated with impaired memory performance (Kumar et al., 2017). Therefore, understanding the underlying mechanisms of PFC dysfunction is crucial to designing practical diagnosis tools and interventions in early AD. Very little attention has been paid so far to the changes in neurometabolites in the PFC in MCI and AD patients. Thus, the current study examines the brain metabolite concentrations in one of the PFC areas distinguished as the working memory region, the left dorsolateral prefrontal cortex (DLPFC), and examines whether changes in neurometabolites are related to the cognitive performance in aMCI patients and healthy older adults.

The neurometabolites are predominantly localized intracellularly, and some metabolites are cell specific (Palombo et al.,2018). For example, recent evidence suggests that high concentration of NAA is found in certain neuronal cell bodies, and thus NAA is considered specific to the neuronal intracellular compartment (Nordengen et al., 2015). Also, NAA is the acetylated form of the amino acid aspartate and becomes one of the most abundant metabolites in the central nervous system (CNS) (Neale et al., 2000, Moffett et al., 2007). Thus, NAA can be used as a disease biomarker for neuronal functioning due to its role in energy production from neuronal mitochondria (Moffett et al., 2007). Another metabolite with high compartmental specificity is myoinositol (mI). mI is a prominent marker for glial cells in the brain and plays a role in cellular signal transduction, osmoregulation, and detoxification. In the CNS, mI has been shown to be primarily localized in astrocytes (Choi et al., 2007). This provides, in principle, a very elegant counterpart to NAA's neuronal preponderance, as mI represents the complementary central intracellular compartment in the CNS. Thus, alterations of these brain metabolite levels could play a pivotal role as mediators of pathological processes observed in AD and MCI (Shonk et al., 1995; Adalsteinsson et al., 2000; De Souza et al., 2011).

Alterations in neurometabolites during disease pathogenesis are also correlated with microstructural properties of brain tissue (Caprihan et al., 2015). However, little is known about the association between the level of neurometabolites and cortical microstructural properties in aging and AD. Recent advances in multi-shell diffusion magnetic resonance imaging (dMRI) offer a unique insight into tissue microstructure (Lampinen et al., 2017; Gozdas et al., 2021). The most promising feature is quantifying neurite (dendrites and axons) density and complexity *in vivo* using the neurite orientation dispersion and density imaging (NODDI) method (Kodiweera et al., 2016). NODDI provides the estimation of intracellular volume fraction (neurite density, ICVF), neurite fanning (ODI), and extracellular volume fraction (free water, ISOVF) (Zhang et al., 2012). However, these water-based diffusion measurements do not provide compartment-specific details of brain tissue. Integrating these tissue properties with neurometabolites will provide unique cell-specific information on the structure of the brain tissue, which has not been studied in older adults and AD. This study will provide more comprehensive information of brain microstructure by integrating the multi-shell dMRI and the neurometabolites to examine the association between ICVF, ODI, and ISOVF with neurometabolites in the left DLPFC. Thus, the neurometabolites will serve as early AD biomarkers with enhanced specificity of tissue microstructures.

In this study, MRS neurometabolites were acquired in individuals with amnestic MCI (aMCI) and healthy older adults in the left DLPFC. aMCI is a subclassification of MCI that focuses specifically on MCI cases involving memory deficits with higher rates of conversion to AD (Griffith et al., 2006). We first aimed to examine the differences in levels of the neural marker NAA, osmolyte, and glial marker mI, the neurotransmitters GABA, the glutamate and glutamine complex Glx relative to total creatine (tCr = Cr + PCr), and the combined NAA/mI and NAA/Glx between aMCI patients and healthy older adults. Then, we explore the associations between neurometabolites with neurite microstructures and with cognitive functions affected in aMCI. Combining the brain metabolite levels with neurite microstructures and cognitive measurements is a step toward clarifying cell and compartment-specificity of brain microstructures and explaining the link between changes in neurometabolite levels and cognitive decline in aMCI patients.

2. Materials and methods

2.1. Participants

Forty-two healthy older adults and 19 aMCI patients were determined to meet inclusion criteria and were enrolled in the study. For these participants, baseline cognitive, neuropsychological, and neuroimaging data were collected in a series of two visits. Patients who fit the inclusion criteria were invited to Stanford University to complete the informed consent procedures as approved by the Stanford Institutional Review Board and undergo the visits. Particularly, participants were administered a series of cognitive and behavioral screening assessments in order to evaluate their mental status. The inclusion criteria for the Healthy Control (HC) group included the following: Age >=65 and <= 85 years old, free of memory complaints, normal memory function (Logical Memory II subscale cutoff score of >=9, >=5 and >=3 for 16, 8–15 and 0–7 years of education, respectively), cognitively normal (absence of significant impairment in cognitive functions and intact Instrumental Activities of Daily Living), Clinical Dementia Rating of 0, Mini Mental-State Examination score >=24.

The inclusion criteria for the aMCI group included the following: age >= 65 and <= 85 years old, diagnosis of amnestic aMCI in the past year (cognitive concern by subject, informant or physician, impairment in memory domain (delayed recall of one paragraph from Logical Memory II subscale from Wechsler memory Scale (Wechsler, 1945) –Revised with cutoff scores of <=8, <=4 and <=2 for 16, 8–15 and 0–7 years of education), absence of dementia, essentially normal functional activities (intact Instrumental Activities of Daily Living (IADL) (Katz et al., 1970), Clinical Dementia Rating (CDR) of 0.5 (Memory Box score of at least 0.5), and Mini-Mental State Examination (MMSE) scores >=24), Hachinski Ischaemic Score <= 4, stability of permitted medications (e.g. cholinesterase inhibitors, hypertension medication, etc.) for at least two months, no Axis I disorder as assessed by the Mini International Neuropsychiatric Interview (Sheehan et al., 1998). Exclusion criteria for both groups in this study included: presence of suicidality, current regular use of psychiatric medications, opiates, or thyroid medications, claustrophobia, non-MRI-compatible materials, current substance abuse, post- traumatic or psychotic disorders, bipolar disorder, any significant neurologic disease, including possible and probable dementia, multi-infarct dementia, Parkinson's or Huntington's disease, brain tumor, progressive supranuclear palsy, seizure disorder, subdural hematoma, multiple sclerosis, "uncontrolled" hypertension, history of significant head trauma, history of alcohol or substance abuse or dependence within the past two years, or any significant systemic or unstable medical condition which could lead to difficulty complying with the training protocol. The study was approved by the Stanford University Institutional Review Board and all participants provided written informed consent.

2.2. NIH Toolbox battery

The National Institute of Health (NIH) Toolbox Cognition domain (nihtoolbox.org) is a battery of tasks performed on an iPad that allows for quick assessment of various domains of cognitive function

(Weintraub et al. 2013). With high test–retest reliability and national standardization of outcomes, this test battery provides reliable measures of cognitive processes across various population samples. Participants completed the NIH Toolbox battery during the second study visit. The battery comprised of several tests including Auditory Verbal Learning Test (Rey) (Dikmen et al., 2014) for testing memory recall and Symbol Digit Modalities Test (SDMT) (Weintraub et al., 2013) for assessing processing speed, and generated Cognitive Fluid composite scores. The Rey test involves auditory presentation of a list of unrelated words and asks participants to immediately recall as many words as possible following the presentation of the words. The SDMT consists of a series of nine symbols presented at the top of a standard sheet of paper, each paired with a single digit. The rest of the sheet contains symbols not matched to a digit, and participants were asked to say the digit corresponding with each symbol as quickly as possible and without making mistakes. The resulting score is equal to the number of correct matches over a period of 120 seconds.

2.3. Neuroimaging data acquisition

The last part of the second study visit involved the participants receiving a magnetic resonance imaging (MRI) scan. All MRI data were acquired on a 3 T GE system (General Electric Healthcare, Milwaukee, WI, USA) equipped with a 32-channel head coil (Nova Medical, Wilmington, MA, USA) at the Center for Cognitive and Neurobiological Imaging at Stanford University (http://www.cni.stanford.edu/). T1-weighted images were performed using 450 ms inversion time (TI), 12-degree flip angle 1 mm slice thickness. MRS was acquired using a modified GE Healthcare PRESS product sequence, PROBE-p™. Two features were added to the product PROBE-p™ sequence for improved localization: (1) 16 step phase cycling (EXORCYCLE on the two refocusing RF pulses) and (2) application of a sensitive point echo-planar (EP) waveform during acquisition to further eliminate out-of-slice artifact in the logical z-direction (Bodenhausen et al., 1977; Gu et al., 2018; Webb et al., 1994). We performed single voxel spectroscopy using this sequence with TE/TR = 35 ms/2s, 64 averages, ~3 minutes of total scan time. The 18x18x18 mm^3 (5.832 mL) single voxel was prescribed in the left dorsolateral prefrontal cortex localized from the 3D T1-weighted anatomical image (see Fig. 1) using a semi-automated voxel placement procedure to place the voxel and applying non-linear normalization to the Montreal Neurological Institute (MNI) space. During the semi-automated voxel placement procedure, the MRS voxel was aligned to the angle of the skull in the sagittal plane, and then the left DLPFC mask in MNI standard space was co-registered to the subject's T1-weighted image. The voxel was manually transcribed to the center of the mask based on each participant's anatomical landmarks (Bishop et al., 2021). dMRI was acquired using a multiband echo-planar imaging (*EPI*) acquisition scheme (multiband factor of 3, MB = 3). Multi-shell dMRI data were acquired for all participants, with isotropic 2.0 mm3 spatial resolution in 80 diffusion directions with diffusion gradient strength set to b = 2855 s/mm^2 and 30 diffusion directions with diffusion gradient strength b = 710 s/mm^2. Each dMRI image also contained nine images without diffusion weighting (b = 0 s/mm^2). An additional scan was acquired in the opposite phase encoding direction consisting of 6 diffusion directions (b = 2855 s/mm^2) and two non-diffusion-weighted images for *EPI* distortion correction. Other dMRI parameters were as follows; TR/TE = 2800/78 ms, matrix size = 112x112, and 63 axial slices.

2.4. Neuroimaging data analysis

Concentrations of NAA, mI, Glx and GABA were quantified and expressed as ratios to total creatine (i.e., creatine and phosphocreatine) levels using the LCModel (Provencher, 2001), which models the *in vivo* spectrum as a linear combination of basis *in vitro* spectra from individual metabolites. Studies have found the collective levels of Cr and PCr to remain relatively stable over long periods, making it useful as a baseline comparison for other metabolite concentrations (Caramanos et al., 2005). Segmentation of the T1-weighted anatomical images into grey matter, white matter, and CSF was performed in the single MRS voxel using SPM12 (https://www.fil.ion.ucl.ac.uk/spm/) (Friston, 2007). dMRI preprocessing was implemented in FSL (fsl.fmrib.ox.ac.uk/fsl/fslwiki/) and MRTrix3(mrtrix.org) and included denoising, geometric *EPI* distortion correction (FSL's topup function), eddy current distortion correction, slice-by-slice motion correction and outlier detection and bias field correction (ANTs N4BiasField Correction). Diffusion gradients were then adjusted to account for the rotation applied to the measurements during motion correction for further analysis (Leemans and Jones, 2009). NODDI coefficients were computed using the NODDI toolbox (https://www.nitrc.org/projects/noddi_toolbox/) in the MATLAB environment. NODDI offers estimates of neurite density (intracellular volume fraction; ICVF), extra-cellular water diffusion (free water) and orientation dispersion index (ODI). The NODDI parameters were computed in the MRS voxel in the left DLPFC by co-registering the T1-weighted and b0 diffusion images.

2.5. Statistical analysis

All statistical analyses were carried out in R studio (version 3.5.3). For each metabolite, one way analysis of covariance was performed on the entire group after exclusion of one healthy older adult and one aMCI for being outliers and including age, sex, gray matter volume, and free water content as covariates. To compute relationships between the left DLPFC neurochemical levels and neurite microstructures and cognitive

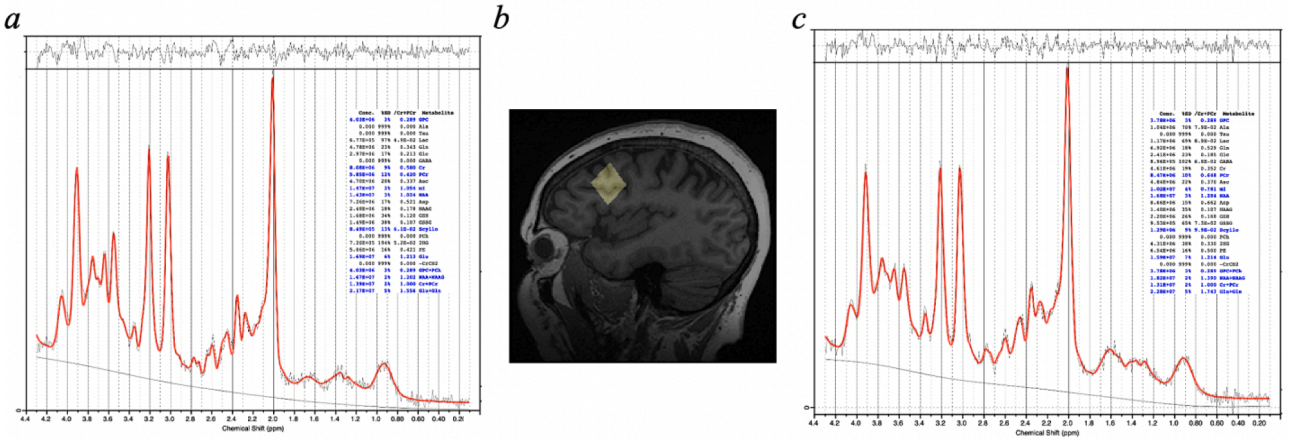

Fig. 1. Representative spectra for one aMCI patient and healthy control (a, c) and voxel placement in the left DLPFC (b).

scores, separate multiple linear regression analyses were performed between NIH cognitive scores, ICVF and ODI and each brain metabolite, where age, sex, gray matter tissue fraction and free water were included as covariates. Benjamini-Hochberg false discovery rate (FDR) correction was used to account for multiple comparisons for one way analysis of covariance and multiple regression analysis ($p_{FDR} < 0.05$).

3. Results

3.1. Participant characteristics

Descriptive statistics and neurocognitive scores are summarized in Table 1. Participants with aMCI had significantly lower MMSE ($p = 0.005$), Auditory Verbal Learning Test (Rey) ($p < 0.001$), Symbol Digit Modalities Test (SDMT) ($p = 0.001$), and Cognitive Fluid composite test ($p = 0.002$) scores. Age and level of education were not significantly different between aMCI and HC. Sex was significantly different between groups and was included as a covariate in statistical analyses.

3.2. Left DLPFC neurometabolites altered in aMCI patients

Significant group differences between healthy controls (HC) and aMCI patients were revealed in the level of neurometabolites in the left DLPFC. aMCI patients had significantly lower levels of NAA/ tCr ($p_{FDR} = 0.04$) and Glx/ tCr ($p_{FDR} = 0.034$) and higher mI/ tCr ($p_{FDR} = 0.04$) when age, sex, gray matter, and free water content were included as covariates (Fig. 2). aMCI patients also showed lower GABA/ tCr compared with HC, but it was not statistically significant.

Further, previous studies suggest that the NAA/ml ratio can be used as an early biomarker for indicating individuals at risk for developing clinical AD (Waragai et al., 2017), and that NAA/Glx ratios may signal altered gluamatergic metabolism while correcting for the effects of neuronal loss as indexed by NAA (Azevedo et al., 2014). Thus, we also evaluated between-group differences in NAA/mI and NAA/Glx ratios and found that NAA/mI significantly decreased in aMCI ($p_{FDR} = 0.01$) (Fig. 1) while the NAA/Glx ratio was not significantly different between groups.

3.3. Neurometabolite associations with age and neurite microstructures

We first examined the effects of aging on brain metabolites in the left DLPFC in the HC and aMCI. A significant negative correlation between age and NAA/tCr was found (Fig. 3a) ($p = 0.02$, uncorrected) in healthy older adults while the NAA/ tCr ratio was not correlated with age in aMCI. Correlations between age and other metabolites did not reach statistical significance ($p > 0.05$) within aMCI and HC groups. We next probed how the left DLPFC neurometabolites were associated with neurite parameters in healthy older adults and aMCI patients and performed an exploratory analysis to test whether age moderates the results. We observed a positive association between NAA/tCr and the neurite density (ICVF) ($p_{FDR} = 0.03$) and a negative association between mI/tCr and neurite complexity/fanning (ODI) ($p_{FDR} = 0.032$) (Fig. 3b and 3c) in healthy older adults. There were no significant associations between any of the neurometabolites and isotropic volume fraction (free water) in HC. No significant correlations were observed between neurometabolites and neurite microstructures in aMCI patients.

While the association between age and ICVF was significant in HC, the relationship between NAA/tCr and ICVF was not significantly mediated by age ($p = 0.08$), suggesting that the relationship of ICVF with NAA/tCr was not obscured by taking the age into account.

Table 1
Demographic, clinical, and neuropsychological characteristics of the sample.

	HC N = 42	aMCI N = 19	Statistics*
Age, years (SD)	73.31 ± 5.58	74.55 ± 6.07	$p = 0.85$
Gender (F/M)	30/12	12/7	$p = 0.02$
Years of Education (SD)	17.88 ± 3.5	18.55 ± 3	$p = 0.44$
MMSE (SD)	28.97 ± 1.05	27.26 ± 1.7	$p = 0.005$
SDMT (SD)	72.06 ±16.6	57.3 ± 10.59	$p = 0.001$
Cognitive Fluid (SD)	90.8 ±9.7	81.8 ±13.2	$p = 0.002$
Rey (SD)	22.27 ±5	16.6 ±5.4	$p < 0.001$

* p values derived from two-sample *t*-test, Chi-square test or ANOVA with age, gender, and education as covariates. HC: Healthy Control; aMCI: amnestic Mild Cognitive Impairment; MMSE: Mini-Mental State Examination; SDMT: Symbol Digit Modalities Test; Rey: Auditory Verbal Learning Test).

3.4. Relationship between neurometabolites and cognitive scores

To investigate whether changes in brain metabolites were accompanied by measurable changes in cognitive performance, we examined the association between the left DLPFC brain metabolites and cognitive scores as assessed via SDMT, Rey's Auditory Verbal Learning Test (Rey) as well as Cognitive Fluid scores in aMCI and healthy older adults. Significant positive associations were observed between NAA/tCr and SDMT, Glx/tCr and SDMT, and NAA/tCr and Cognitive Fluid cognitive scores in the combined group (aMCI plus healthy older adults) ($p_{FDR} < 0.05$) (Fig. 4). These correlations, however, were not robust within each group. Only a significant positive correlation was found between Glx/tCr and SDMT within HC. In addition, significant group differences were observed in the associations between Rey scores with Glx/tCr ($p_{FDR} = 0.01$) and GABA/tCr ($p_{FDR} = 0.017$). However, these associations were not significant within groups. Finally, the NAA/mI ratio was positively correlated with Cognitive Fluid ($p_{FDR} = 0.014$) and Rey ($p_{FDR} = 0.014$) in the combined group.

4. Discussion

This research investigated the changes in brain metabolite levels in the left DLPFC between healthy older subjects and aMCI patients and their relationship with measures of neurite microstructures and cognitive functioning. We found that aMCI patients have impaired brain metabolite levels in the left DLPFC compared with healthy older individuals, and that impaired left DLPFC neurometabolites levels were associated with lower cognitive scores. To our knowledge, this study demonstrates for the first time the associations between brain metabolites and neurite parameters (ICVF and ODI) measured in the left DLPFC in older adults, and these associations were not significant in aMCI patients. The results of this study extend current knowledge on disturbed brain metabolites in PFC in aMCI and allow for characterization of cell-specific properties of brain microstructures by probing the associations between changes in microstructural properties and metabolite concentrations in older age.

The previous work showed that reduced NAA is an indicator of neuronal loss, and increased mI likely indicates glial activation and inflammation linked to AD neuropathology (Waragai et al., 2017; Voevodskaya et al., 2016). Also, decreased levels of NAA and increased levels of mI in several brain areas are highly associated with AD disease progression (Voevodskaya et al., 2019). These classic hallmarks of MCI and AD pathophysiology are mainly reported in the ACC and PCC because these regions are vulnerable to amyloid-β plaques (Aβ) development (Small et al., 2006; Pike et al., 2007). However, several recent studies reported deficits in DLPFC neuroplasticity that could play a positive role in cognitive decline and a low level of endogenous amyloid (Kumar et al., 2017) and network dysfunctions in DLPFC in AD patients. In this study, we investigated the metabolite levels in the left DLPFC, and the patients with aMCI showed lower levels of NAA/ tCr and higher mI/ tCr compared with healthy older adults, which may signal inflammatory and neurodegenerative processes in the early stages of AD.

Changes in the glutamate and glutamine complex Glx and GABA neurometabolite levels have also been frequently studied in MCI and AD (Friedman et al., 2013; Huang et al., 2017; Oeltzschner et al., 2019).

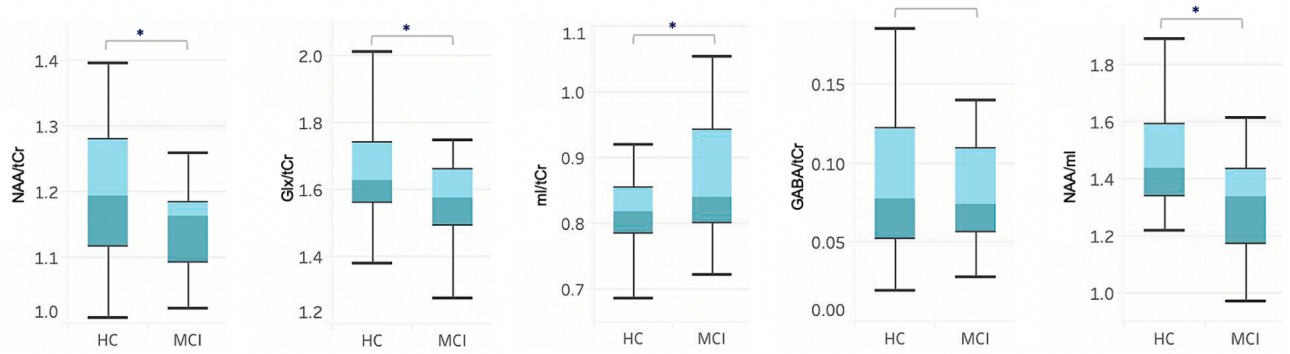

Fig. 2. Neurometabolites in the left DLPFC. In the left DLPFC, concentrations of NAA/tCr, Glx/tCr and NAA/mI were significantly lower and mI/tCr was significantly higher in aMCI patients than healthy controls (* p values are FDR corrected < 0.05). The line between dark green and light green states the median value of the metabolites in each group.

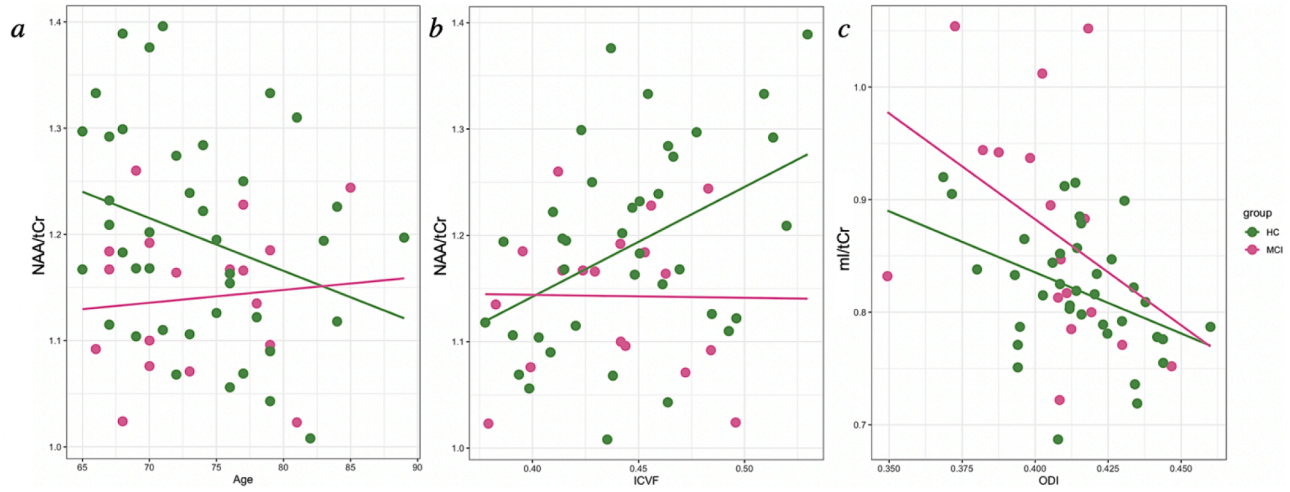

Fig. 3. Age and neurite microstructural characteristics associated with brain metabolites in the left DLPFC in healthy older adults and aMCI patients. (a) Age and NAA/tCr were significantly correlated in healthy older adults (p = 0.02, uncorrected). (b, c) NAA/tCr and the neurite density (ICVF) (p_{FDR} = 0.03), and mI/tCr and neurite complexity/fanning (ODI) (p_{FDR} = 0.032) were significantly associated in healthy older adults.

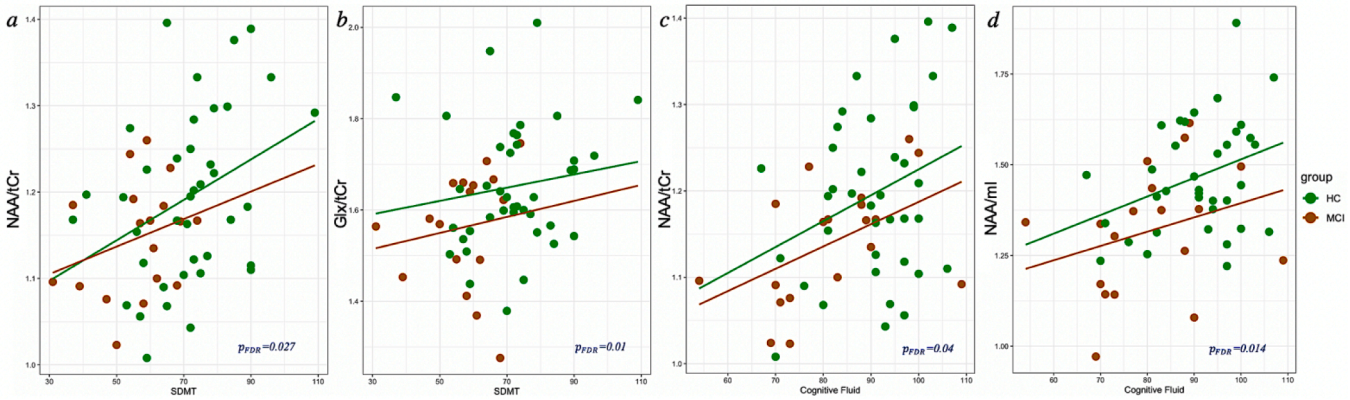

Fig. 4. Correlations between the left DLPFC brain metabolites and cognitive scores in aMCI and healthy older adults. (a, b) NAA/tCr, Glx/tCr and SDMT; (c, d) NAA/tCr, the NAA/mI ratio are positively correlated with Cognitive Fluid (p_{FDR} < 0.05) in the combined group. SDMT: Symbol Digit Modalities Test.

However, these studies have shown mixed findings regarding the potential changes in the GABA and Glx complex in MCI and AD. Particularly, decreased levels of Glx and GABA have not been long established in MCI and AD patients. One recent study showed decreased Glx in the posterior cingulate while other studies reported no changes in MCI, while patients with AD showed decreased Glx in the posterior cingulate and hippocampus (Fayed et al., 2011; Rupsingh et al., 2011). Similarly, one recent study found significantly lower levels of GABA in AD patients in the posterior but not the anterior cingulate (Bai et al. ,2015), while another recent study at 7 T field strength showed decreased GABA in MCI patients both in the anterior and posterior cingulate (Riese et al., 2015; Oeltzschner et al., 2019). Together, the lower left DLPFC Glx

levels observed in the current study in aMCI patients is in line with the previous findings. However, our results did not support lower levels of GABA in aMCI. This discrepancy can be explained by the relatively strong Glx combined signal that is easily detectable at lower field strengths, whereas detecting changes in GABA signal may require a higher magnetic field strength (Oeltzschner et al., 2019, Shungu et al., 2016).

Further, considering that the ratio of brain metabolite concentrations may be more sensitive to metabolic disruptions of related molecules than the concentration of a single metabolite alone (Lewis et al., 2020), we also found that the NAA/ml ratio was significantly decreased in aMCI compared to healthy older adults. Lower NAA/mI has been shown to predict progression from HC to MCI and was correlated with both higher tau and *Aβ* levels (Murray et al., 2014). One recent study also demonstrated the utility of composite NAA/mI ratio as a marker of increased longitudinal *Aβ* accumulation in HC older adults (Nedelska et al., 2017). Similarly, a longitudinal study (Voevodskaya et al., 2019) examined the association between longitudinal changes in proton MRS metabolites in the midsagittal PCC/precuneus and amyloid pathology and found that Aβ positive (Aβ +) individuals with low baseline NAA/mI had a significantly higher rate of cognitive decline than Aβ + individuals with high baseline NAA/mI. They also concluded that the longitudinal change in NAA/mI was associated with underlying amyloid pathology and could be relevant for predicting a worsening of cognitive symptoms. Moreover, NAA/mI has been suggested as an early marker of neurodegeneration, distinguishing AD patients from other patient groups and predicting the progression from MCI to AD at two year follow-ups (Mitolo et al., 2019; Mitolo et al., 2021). Thus, the lower NAA/mI in aMCI may offer an early insight into dynamic disease biomarkers during the pre-dementia stages of AD.

Previous evidence also suggests that the brain metabolite system plays an essential role in cognitive functioning (Pfleiderer et al., 2004; Patel et al., 2014). A few recent studies have revealed associations between metabolite levels in the PCC and ACC with performance in California Verbal Learning Test (CVLT) and verbal fluency tests in MCI patients (Oeltzschner et al., 2019; Mandal et al., 2015). However, the association between ^{1}H-MRS metabolites and cognitive deficits in aMCI is not clear. Here, we found significant associations between NAA/tCr and Glx/tCr with SDMT scores, and between NAA/tCr and NAA/mI ratios and Cognitive Fluid scores in the combined group, and the correlations between Rey scores with Glx/tCr and GABA/tCr were significantly different between groups. The cognitive and memory scores were also significantly different between aMCI and healthy older adults. These results suggest that 1H-MRS metabolite levels in the DLPFC are significantly correlated with decline in memory and executive functioning that further support the potential of these metabolites as biomarkers to detect cognitive decline in aMCI at an early stage.

Recent advances in dMRI provide more specific markers of brain tissue microstructure by estimating the density and complexity of neurite structure in brain tissue (Zhang et al., 2012). In this study, we also investigated the specificity of dMRI parameters to detecting neurochemical changes measured in the left DLPFC. It should be noted that the present study is the first to examine the association between the left DLPFC neurometabolite levels and neurite properties in healthy older adults and aMCI patients. A few studies have previously investigated the relationship between conventional white matter parameters (e.g., FA) and brain metabolites in healthy older adults and patients with schizophrenia and mild traumatic brain injury (Caprihan et al., 2015; Grossman et al., 2015; Reid et al., 2016). One of these studies also reported a positive association between NAA and intra-axonal diffusivity in patients with mild traumatic brain injury (Grossman et al., 2015). Here, we observed a positive correlation between ICVF and NAA/tCr and a negative correlation between ODI and mI/tCr in older adults, while these correlations were not statistically significant in patients with aMCI. These data suggest a potential decoupling in the relationship between neurite microstructures and NAA/tCr and mI/tCr concentrations in DLPFC in the early stage of AD, but this also needs to be confirmed in future studies. While the studied neurite parameters provide useful information regarding intra-cellular volume fraction and angular variation of neurite orientation in brain tissue, ^{1}H-MRS provides complementary and more sensitive information regarding biochemical properties of the tissue. For example, NAA is an endogenous probe of the neuronal intracellular compartment (Kroenke et al., 2004) that also presents in oligodendrocytes which are predominant in white matter and responsible for covering neurons with an insulator material called myelin (Rae, 2014). NAA also reflects non-structural pathophysiology such as mitochondrial impairment, to which diffusion parameters are not sensitive (Li et al., 2013). Similarly, mI comprises glial cells responsible for many functions, including supporting neurons, helping repair damage to nervous system tissue, and regulating communication between neurons (Sheikh-Bahaei, 2020). Thus, the observed correlations between NAA/tCr and ICVF and mI/tCr and ODI in our study provide early evidence regarding the sensitivity of advanced diffusion parameters to neurometabolite levels *in vivo* and elucidates the potential biophysical mechanisms that influence structural and metabolic changes in older adults and aMCI patients.

However, the study is limited because of the relatively small aMCI sample and the generalizability of the results is somewhat limited. It should also be noted that there was a significant difference in sex between aMCI and control groups, and sex was therefore included as a covariate in the group analysis of metabolite levels and correlation analyses. Future studies with a larger sample size of aMCI patients, sex-matched patient and control groups, longitudinal follow-ups, as well as utilizing the absolute brain metabolite concentrations other than using the ratios (e.g., relative to total creatine) will allow us to corroborate these findings and elucidate the impact of each brain metabolite's role in predicting the possible progression to AD. Future studies investigating longitudinal changes in aMCI-related brain metabolites are needed to better understand whether the results can be generalized to clinical practice.

In conclusion, our data provide further insight into changes in brain metabolites in aMCI patients. Particularly, we found decreased NAA, mI, Glx, and NAA/mI ratio in the left DLPFC in aMCI that provides useful insights regarding neurometabolic changes in prodromal stage of AD. We also found a significant association between DLPFC metabolite levels and Cognitive Fluid scores that suggests a link between disturbance in neurotransmission and cognitive deficits in early stages of AD. We also examined the relationship between the neurometabolites and advanced diffusion measures in healthy older adults and aMCI and observed significant correlations between NAA and mI with measures of neurite density and complexity. These results provide first-hand evidence regarding the relationship between the diffusion parameters and neurometabolites in the left DLPFC that may further explain mechanisms underlying cognitive decline in aMCI. Overall, our data suggest that the left DLPFC metabolites can ascertain differences in aMCI patients compared with controls, are associated with neurite properties in healthy aging, and predict possible deficits in cognitive performance in the prodromal stage of AD.

Declaration of Competing Interest

The authors declare that they have no known competing financial interests or personal relationships that could have appeared to influence the work reported in this paper.

Data availability

The data are not publicly available due to privacy issues of clinical data.

Acknowledgements

We thank the participants for their involvement in the study as well as the researchers involved in coordinating data collection for this project. We also thank Laima Baltusis and Hua Wu for their inputs on the imaging procedures.

Author contributions

E.G. contributed to MRI data collection, carried out image processing and statistical analysis, and drafted the manuscript. L.H, H.F. and L.D. contributed to recruitment, study design and coordination, behavioral data collection, MRI data collection and drafting the manuscript. M.G., M.S. and R.H. contributed to study design and drafting the manuscript. S.M.H. conceived of the study, participated in its design and coordination, and helped with drafting the manuscript. All authors read and approved the final manuscript.

Funding

The study was partly funded by a Career Development Award from the National Institute on Aging (NIA) to SMH (K25AG050759). EG's effort was partly supported by Stanford Maternal and Child Health Research Institute (MCHRI). SMH's effort was supported in part by NIA (K25AG050759, R01AG073362, R01AG072470, R21AG073973 and R21AG064263) and National Institute of Mental Health (NIMH) (R61MH119289, R21MH123873 and R21AG073973).

References

Adalsteinsson, E., Sullivan, E.V., Kleinhans, N., Spielman, D.M., Pfefferbaum, A., 2000. Longitudinal decline of the neuronal marker N-acetyl aspartate in Alzheimer's disease. The Lancet 355 (9216), 1696–1697.

Azevedo, C.J., Kornak, J., Chu, P., Sampat, M., Okuda, D.T., Cree, B.A., Nelson, S.J., Hauser, S.L., Pelletier, D., 2014. In vivo evidence of glutamate toxicity in multiple sclerosis. Ann. Neurol. 76 (2), 269–278.

Bai, X., Edden, R.A.E., Gao, F., Wang, G., Wu, L., Zhao, B., Wang, M., Chan, Q., Chen, W., Barker, P.B., 2015. Decreased γ-aminobutyric acid levels in the parietal region of patients with Alzheimer's disease. J. Magn. Reson. Imaging 41 (5), 1326–1331.

Bishop, J.H., Geoly, A., Khan, N., Tischler, C., Krueger, R., Amin, H., Baltusis, L., Wu, H., Spiegel, D., Williams, N., 2021. Real-Time Semi-Automated and Automated Voxel Placement for Repeated Acquisition Magnetic Resonance Spectroscopy. medRxiv.

Bodenhausen, G., Freeman, R., Turner, D.L., 1977. Suppression of artifacts in two-dimensional J spectroscopy. J. Magn. Reson. 27 (3), 511–514.

Caprihan, A., Jones, T., Chen, H., Lemke, N., Abbott, C., Qualls, C., Canive, J., Gasparovic, C., Bustillo, J.R., 2015. The paradoxical relationship between white matter, psychopathology and cognition in schizophrenia: a diffusion tensor and proton spectroscopic imaging study. Neuropsychopharmacology 40 (9), 2248–2257.

Caramanos, Z., Narayanan, S., Arnold, D.L., 2005. 1H-MRS quantification of tNA and tCr in patients with multiple sclerosis: a meta-analytic review. Brain 128, 2483–2506.

Choi, J.-K., Dedeoglu, A., Jenkins, B.G., 2007. Application of MRS to mouse models of neurodegenerative illness. NMR in Biomedicine 20 (3), 216–237.

De Souza, A.S., de Oliveira-Souza, R., Moll, J., Tovar-Moll, F., Andreiuolo, P.A., Bottino, C.M., 2011. Contribution of 1H spectroscopy to a brief cognitive-functional test battery for the diagnosis of mild Alzheimer's disease. Dement. Geriatr. Cogn. Disord. 32, 351–361.

Dikmen, S.S., Bauer, P.J., Weintraub, S., Mungas, D., Slotkin, J., Beaumont, J.L., Gershon, R., Temkin, N.R., Heaton, R.K., 2014. Measuring episodic memory across the lifespan: NIH toolbox picture sequence memory test. J. Int. Neuropsychological Soc. 20 (6), 611–619.

Dubois, B., Villain, N., Frisoni, G.B., Rabinovici, G.D., Sabbagh, M., Cappa, S., Bejanin, A., Bombois, S., Epelbaum, S., Teichmann, M., Habert, M.-O., Nordberg, A., Blennow, K., Galasko, D., Stern, Y., Rowe, C.C., Salloway, S., Schneider, L.S., Cummings, J.L., Feldman, H.H., 2021. Clinical diagnosis of Alzheimer's disease: recommendations of the International Working Group. Lancet Neurology 20 (6), 484–496.

Eichenbaum, H., 2017. Prefrontal–hippocampal interactions in episodic memory. Nat. Rev. Neurosci. 18 (9), 547–558.

Fayed, N., Modrego, P.J., Rojas-Salinas, G., Aguilar, K., 2011. Brain glutamate levels are decreased in Alzheimer's disease: a magnetic resonance spectroscopy study. Am. J. Alzheimer's Disease Other Dementias 26 (6), 450–456.

Friedman, S.D., Baker, L.D., Borson, S., Jensen, J.E., Barsness, S.M., Craft, S., Merriam, G. R., Otto, R.K., Novotny, E.J., Vitiello, M.V., 2013. Growth Hormone-Releasing Hormone effects on brain γ-Aminobutyric acid levels in mild cognitive impairment and healthy aging. JAMA neurology 70, 883–890.

Friston, K., 2007. A short history of SPM. Statistical parametrical mapping: The analysis of functional brain images, 3-9.

Gao, F., Barker, P.B., 2014. Various MRS application tools for Alzheimer disease and mild cognitive impairment. American journal of neuroradiology 35 (Supplement 6), S4–S11.

Govindpani, K., Turner, C., Waldvogel, H.J., Faull, R.L., Kwakowsky, A., 2020. Impaired expression of GABA signaling components in the Alzheimer's disease middle temporal gyrus. Int. J. Mol. Sci. 21, 8704.

Gozdas, E., Fingerhut, H., Wu, H., Bruno, J.L., Dacorro, L., Jo, B., O'Hara, R., Reiss, A.L., Hosseini, S.M.H., 2021. Quantitative measurement of macromolecular tissue properties in white and gray matter in healthy aging and amnestic MCI. Neuroimage 237, 118161.

Griffith, H.R., Netson, K.L., Harrell, L.E., Zamrini, E.Y., Brockington, J.C., Marson, D.C., 2006. Amnestic mild cognitive impairment: diagnostic outcomes and clinical prediction over a two-year time period. Journal of the International Neuropsychological Society 12 (2), 166–175.

Grossman, E.J., Kirov, I.I., Gonen, O., Novikov, D.S., Davitz, M.S., Lui, Y.W., Grossman, R.I., Inglese, M., Fieremans, E., 2015. N-acetyl-aspartate levels correlate with intra-axonal compartment parameters from diffusion MRI. Neuroimage 118, 334–343.

Gu, M., Hurd, R., Noeske, R., Baltusis, L., Hancock, R., Sacchet, M.D., Gotlib, I.H., Chin, F.T., Spielman, D.M., 2018. GABA editing with macromolecule suppression using an improved MEGA-SPECIAL sequence. Magn. Reson. Med. 79 (1), 41–47.

Huang, D., Liu, D., Yin, J., Qian, T., Shrestha, S., Ni, H., 2017. Glutamate-glutamine and GABA in brain of normal aged and patients with cognitive impairment. Eur. Radiol. 27 (7), 2698–2705.

Jessen, F., Gur, O., Block, W., Ende, G., Frolich, L., Hammen, T., Wiltfang, J., Kucinski, T., Jahn, H., Heun, R., Maier, W., Kolsch, H., Kornhuber, J., Traber, F., 2009. A multicenter 1H-MRS study of the medial temporal lobe in AD and MCI. Neurology 72 (20), 1735–1740.

Jones, R.S., Waldman, A.D., 2004. 1H-MRS evaluation of metabolism in Alzheimer's disease and vascular dementia. Neurol. Res. 26, 488–495.

Jung, Y.H., Park, S., Jang, H., Cho, S.H., Kim, S.J., Kim, J.P., Kim, S.T., Na, D.L., Seo, S. W., Kim, H.J., 2020. Frontal-executive dysfunction affects dementia conversion in patients with amnestic mild cognitive impairment. Sci. Rep. 10, 1–8.

Kantarci, K., 2013. Proton MRS in mild cognitive impairment. J. Magn. Reson. Imaging 37 (4), 770–777.

Katz, S., Downs, T.D., Cash, H.R., Grotz, R.C., 1970. Progress in development of the index of ADL. The gerontologist 10 (1 Part 1), 20–30.

Kodiweera, C., Alexander, A.L., Harezlak, J., McAllister, T.W., Wu, Y.-C., 2016. Age effects and sex differences in human brain white matter of young to middle-aged adults: A DTI, NODDI, and q-space study. Neuroimage 128, 180–192.

Kroenke, C.D., Ackerman, J.J.H., Yablonskiy, D.A., 2004. On the nature of the NAA diffusion attenuated MR signal in the central nervous system. Magnetic Resonance in Medicine 52 (5), 1052–1059.

Kumar, S., Zomorrodi, R., Ghazala, Z., Goodman, M.S., Blumberger, D.M., Cheam, A., Fischer, C., Daskalakis, Z.J., Mulsant, B.H., Pollock, B.G., Rajji, T.K., 2017. Extent of dorsolateral prefrontal cortex plasticity and its association with working memory in patients with Alzheimer disease. JAMA psychiatry 74 (12), 1266.

Lampinen, B., Szczepankiewicz, F., Mårtensson, J., van Westen, D., Sundgren, P.C., Nilsson, M., 2017. Neurite density imaging versus imaging of microscopic anisotropy in diffusion MRI: a model comparison using spherical tensor encoding. Neuroimage 147, 517–531.

Leemans, A., Jones, D.K., 2009. The B-matrix must be rotated when correcting for subject motion in DTI data. Magnetic Resonance in Medicine 61 (6), 1336–1349.

Lewis, C.P., Port, J.D., Blacker, C.J., Sonmez, A.I., Seewoo, B.J., Leffler, J.M., Frye, M.A., Croarkin, P.E., 2020. Altered anterior cingulate glutamatergic metabolism in depressed adolescents with current suicidal ideation. Transl. Psychiatry 10, 1–12.

Li, S., Clements, R., Sulak, M., Gregory, R., Freeman, E., McDonough, J., 2013. Decreased NAA in gray matter is correlated with decreased availability of acetate in white matter in postmortem multiple sclerosis cortex. Neurochem. Res. 38 (11), 2385–2396.

Mandal, P.K., Saharan, S., Tripathi, M., Murari, G., 2015. Brain glutathione levels–a novel biomarker for mild cognitive impairment and Alzheimer's disease. Biol. Psychiatry 78 (10), 702–710.

Maschio, C., Ni, R., 2022. Amyloid and Tau Positron Emission Tomography Imaging in Alzheimer's Disease and Other Tauopathies. Frontiers in aging neuroscience 14.

Mitolo, M., Stanzani-Maserati, M., Capellari, S., Testa, C., Rucci, P., Poda, R., Oppi, F., Gallassi, R., Sambati, L., Rizzo, G., 2019. Predicting conversion from mild cognitive impairment to Alzheimer's disease using brain 1H-MRS and volumetric changes: a two-year retrospective follow-up study. NeuroImage: Clinical 23, 101843.

Mitolo, M., Stanzani-Maserati,, M., Manners, D.N., Capellari, S., Testa, C., Talozzi, L., Poda, R., Oppi, F., Evangelisti, S., Gramegna, L.L., 2021. The Combination of Metabolic Posterior Cingulate Cortical Abnormalities and Structural Asymmetries Improves the Differential Diagnosis Between Primary Progressive Aphasia and Alzheimer's Disease. J. Alzheimers Dis. 82, 1467–1473.

Moffett, J., Ross, B., Arun, P., Madhavarao, C., Namboodiri, A., 2007. N-Acetylaspartate in the CNS: from neurodiagnostics to neurobiology. Prog. Neurobiol. 81 (2), 89–131.

Murray, P.S., Kumar, S., DeMichele-Sweet, M.A.A., Sweet, R.A., 2014. Psychosis in Alzheimer's disease. Biol. Psychiatry 75 (7), 542–552.

Neale, J.H., Bzdega, T., Wroblewska, B., 2000. N-Acetylaspartylglutamate: the most abundant peptide neurotransmitter in the mammalian central nervous system. J. Neurochem. 75, 443–452.

Nedelska, Z., Przybelski, S.A., Lesnick, T.G., Schwarz, C.G., Lowe, V.J., Machulda, M.M., Kremers, W.K., Mielke, M.M., Roberts, R.O., Boeve, B.F., Knopman, D.S., Petersen, R. C., Jack, C.R., Kantarci, K., 2017. 1H-MRS metabolites and rate of β-amyloid accumulation on serial PET in clinically normal adults. Neurology 89 (13), 1391–1399.

Nordengen, K., Heuser, C., Rinholm, J.E., Matalon, R., Gundersen, V., 2015. Localisation of N-acetylaspartate in oligodendrocytes/myelin. Brain Struct. Funct. 220 (2), 899–917.
Novotny, E., Ashwal, S., Shevell, M., 1998. Proton magnetic resonance spectroscopy: an emerging technology in pediatric neurology research. Pediatr. Res. 44 (1), 1–10.
Oeltzschner, G., Wijtenburg, S.A., Mikkelsen, M., Edden, R.A., Barker, P.B., Joo, J.H., Leoutsakos, J.-M.-S., Rowland, L.M., Workman, C.I., Smith, G.S., 2019. Neurometabolites and associations with cognitive deficits in mild cognitive impairment: a magnetic resonance spectroscopy study at 7 Tesla. Neurobiol. Aging 73, 211–218.
Olson, B.L.B., Holshouser, B.A., Britt III, W., Mueller, C., Baqai, W., Patra, S., Petersen, F., Kirsch, W.M., 2008. Longitudinal metabolic and cognitive changes in mild cognitive impairment patients. Alzheimer Dis. Assoc. Disord. 22, 269–277.
Palombo, M., Ligneul, C., Hernandez-Garzon, E., Valette, J., 2018. Can we detect the effect of spines and leaflets on the diffusion of brain intracellular metabolites? Neuroimage 182, 283–293.
Patel, T., Blyth, J.C., Griffiths, G., Kelly, D., Talcott, J.B., 2014. Moderate relationships between NAA and cognitive ability in healthy adults: implications for cognitive spectroscopy. Front. Hum. Neurosci. 8.
Pfleiderer, B., Ohrmann, P., Suslow, T., Wolgast, M., Gerlach, A.L., Heindel, W., Michael, N., 2004. N-acetylaspartate levels of left frontal cortex are associated with verbal intelligence in women but not in men: a proton magnetic resonance spectroscopy study. Neuroscience 123 (4), 1053–1058.
Pike, K.E., Savage, G., Villemagne, V.L., Ng, S., Moss, S.A., Maruff, P., Mathis, C.A., Klunk, W.E., Masters, C.L., Rowe, C.C., 2007. β-amyloid imaging and memory in non-demented individuals: evidence for preclinical Alzheimer's disease. Brain 130, 2837–2844.
Provencher, S.W., 2001. Automatic quantitation of localized in vivo 1H spectra with LCModel. NMR in Biomedicine 14 (4), 260–264.
Rae, C.D., 2014. A guide to the metabolic pathways and function of metabolites observed in human brain 1 H magnetic resonance spectra. Neurochem. Res. 39 (1), 1–36.
Reid, M.A., White, D.M., Kraguljac, N.V., Lahti, A.C., 2016. A combined diffusion tensor imaging and magnetic resonance spectroscopy study of patients with schizophrenia. Schizophr. Res. 170 (2-3), 341–350.
Riese, F., Gietl, A., Zölch, N., Henning, A., O'Gorman, R., Kälin, A.M., Leh, S.E., Buck, A., Warnock, G., Edden, R.A.E., Luechinger, R., Hock, C., Kollias, S., Michels, L., 2015. Posterior cingulate γ-aminobutyric acid and glutamate/glutamine are reduced in amnestic mild cognitive impairment and are unrelated to amyloid deposition and apolipoprotein E genotype. Neurobiol. Aging 36 (1), 53–59.
Rupsingh, R., Borrie, M., Smith, M., Wells, J.L., Bartha, R., 2011. Reduced hippocampal glutamate in Alzheimer disease. Neurobiol. Aging 32 (5), 802–810.
Salat, D.H., Kaye, J.A., Janowsky, J.S., 2001. Selective preservation and degeneration within the prefrontal cortex in aging and Alzheimer disease. Arch. Neurol. 58, 1403–1408.
Sheehan, D.V., Lecrubier, Y., Sheehan, K.H., Amorim, P., Janavs, J., Weiller, E., Hergueta, T., Baker, R., Dunbar, G.C., 1998. The Mini-International Neuropsychiatric Interview (MINI): the development and validation of a structured diagnostic psychiatric interview for DSM-IV and ICD-10. J. Clin. Psychiatry 59, 22–33.
Sheikh-Bahaei, N., 2020. MR spectroscopy in Alzheimer's disease. Biomed. Spectrosc. Imaging 9 (1-2), 13–21.
Shonk, T.K., Moats, R.A., Gifford, P., Michaelis, T., Mandigo, J.C., Izumi, J., Ross, B.D., 1995. Probable Alzheimer disease: diagnosis with proton MR spectroscopy. Radiology 195 (1), 65–72.
Shungu, D.C., Mao, X., Gonzales, R., Soones, T.N., Dyke, J.P., van der Veen, J.W., Kegeles, L.S., 2016. Brain γ-aminobutyric acid (GABA) detection in vivo with the J-editing 1H MRS technique: a comprehensive methodological evaluation of sensitivity enhancement, macromolecule contamination and test–retest reliability. NMR Biomed. 29 (7), 932–942.
Small, G.W., Kepe, V., Ercoli, L.M., Siddarth, P., Bookheimer, S.Y., Miller, K.J., Lavretsky, H., Burggren, A.C., Cole, G.M., Vinters, H.V., Thompson, P.M., Huang, S.-C., Satyamurthy, N., Phelps, M.E., Barrio, J.R., 2006. PET of brain amyloid and tau in mild cognitive impairment. N. Engl. J. Med. 355 (25), 2652–2663.
Spellman, T., Rigotti, M., Ahmari, S.E., Fusi, S., Gogos, J.A., Gordon, J.A., 2015. Hippocampal–prefrontal input supports spatial encoding in working memory. Nature 522 (7556), 309–314.
Squire, L.R., Stark, C.E.L., Clark, R.E., 2004. The medial temporal lobe. Annu. Rev. Neurosci. 27 (1), 279–306.
van Veluw, S.J., Sawyer, E.K., Clover, L., Cousijn, H., De Jager, C., Esiri, M.M., Chance, S. A., 2012. Prefrontal cortex cytoarchitecture in normal aging and Alzheimer's disease: a relationship with IQ. Brain Struct. Funct. 217 (4), 797–808.
Voevodskaya, O., Sundgren, P.C., Strandberg, O., Zetterberg, H., Minthon, L., Blennow, K., Wahlund, L.-O., Westman, E., Hansson, O., 2016. Myo-inositol changes precede amyloid pathology and relate to APOE genotype in Alzheimer disease. Neurology 86 (19), 1754–1761.
Voevodskaya, O., Poulakis, K., Sundgren, P., van Westen, D., Palmqvist, S., Wahlund, L.-O., Stomrud, E., Hansson, O., Westman, E., 2019. Brain myoinositol as a potential marker of amyloid-related pathology: A longitudinal study. Neurology 92 (5), e395–e405.
Waragai, M., Moriya, M., Nojo, T., 2017. Decreased N-acetyl aspartate/myo-inositol ratio in the posterior cingulate cortex shown by magnetic resonance spectroscopy may be one of the risk markers of preclinical Alzheimer's disease: a 7-year follow-up study. J. Alzheimers Dis. 60 (4), 1411–1427.
Webb, P.G., Sailasuta, N., Kohler, S.J., Raidy, T., Moats, R.A., Hurd, R., 1994. Automated single-voxel proton MRS: technical development and multisite verification. Magn. Reson. Med. 31 (4), 365–373.
Wechsler, D., 1945. Wechsler memory scale.
Weintraub, S., Dikmen, S.S., Heaton, R.K., Tulsky, D.S., Zelazo, P.D., Bauer, P.J., Carlozzi, N.E., Slotkin, J., Blitz, D., Wallner-Allen, K., Fox, N.A., Beaumont, J.L., Mungas, D., Nowinski, C.J., Richler, J., Deocampo, J.A., Anderson, J.E., Manly, J.J., Borosh, B., Havlik, R., Conway, K., Edwards, E., Freund, L., King, J.W., Moy, C., Witt, E., Gershon, R.C., 2013. Cognition assessment using the NIH Toolbox. Neurology 80 (Issue 11, Supplement 3), S54–S64.
Zhang, Y., Zou, Q.-P., Greaves, D., 2012. Air–water two-phase flow modelling of hydrodynamic performance of an oscillating water column device. Renewable Energy 41, 159–170.